

Temperature-dependent ultrasonic attenuation of superconducting composite Y123+Ni at low temperature

Hesham A. Afifi¹, Ibrahim Z. Hager², Nadia S. Abdel Aal¹ and Ahmed M. Abd El-Aziz¹

¹(Ultrasonic Laboratory, National Institute for Standards, Egypt)

²(Physics Department, Faculty of Science / Menoufia University, Egypt)

Abstract: A series of superconducting composite (100-x) YBa₂Cu₃O_{7-δ} + x Ni metal (x = 0, 2.5, 5, 10 and 15 wt.%) was prepared using conventional solid state reaction route. The attenuation coefficient (α) of the ultrasonic longitudinal waves at frequency 4MHz was measured for these samples in the temperature range 60-120 K. The results showed the clear effect of Ni²⁺-presence in CuO₂ plane on anti-ferromagnetic (AF) correlations. Increasing Ni²⁺ ions in CuO₂ plane decreases the height of an attenuation peak (P1) in the vicinity of the superconducting transition temperature T_C. Decreases of both P1 and T_C with Ni wt.% were found to have similar trends suggesting that the relaxation species of P1 may be correlated with superconductivity.

Keywords –Superconducting composite, ultrasonic attenuation, relaxation process, anti-ferromagnetic (AF) correlations, Y123, Ni.

Date of Submission: 27-08-2018

Date of acceptance: 09-09-2018

I. INTRODUCTION

Since the discovery of high-T_C superconductivity in cuprates, it has been postulated that CuO₂ planes play the crucial role for the superconducting mechanisms in these compounds [1]. In Ni-doped cuprate superconductors, Ni²⁺ ions mainly substitute the Cu plane sites and such substitution at high-level results in a degradation in superconductivity [2-5]. Ni²⁺ ions doping in Cu-plane sites have two different roles; potential and magnetic scatterings. For increased-Ni-doped cuprates, the marked degradation of the superconducting properties is stated mainly due to potential scattering [6-8]. Ni²⁺ ions alter the hopping integrals, as a result of anti-JT distortions arisen in the cuprate lattice as substituting Cu in CuO₂ plane [9]. The effect of Ni²⁺ as magnetic scatterer is clear in perturbing the anti-ferromagnetic (AF) correlations, superexchange interaction, arising between neighboring localized electrons on Cu-sites via intervening O²⁻ ions [10-12]. Ni²⁺ ions therefore affect the Zhang–Rice singlets and their pairing mechanism which are the key object for high-T_C superconductivity [13]. Anti-ferromagnetism, pairing mechanisms and superconductivity in two-dimensional CuO₂ planes still open to debate. Thus investigating the role of Ni²⁺ ions on AF correlations and their effect on T_C might aid in unveiling the physics of HTSC. For this purpose, we investigated the effects on T_C and dynamic processes made by Ni doping in YBa₂Cu₃O_{7-δ} (Y123) via measuring temperature-dependent ultrasonic attenuation. Measurements of ultrasonic attenuation (α) versus temperature is a non-destructive method and very effective tool for observing and studying many physical processes in cuprate compounds such as the lattice instabilities, phase transitions or relaxation processes associated with the superconducting transition [14-18]. In this work we report the results of α measurements in the temperature range 60-120 K performed on a series of Y123 +Ni samples. The evolution of α peaks with Ni doping is studied and the origin of the suppressing effect of Ni substitution on T_C is discussed.

II. EXPERIMENTAL

2.1. Preparation of samples

Superconducting powder of YBa₂Cu₃O_{7-δ} was prepared from 99.9%-purity powders of Y₂O₃, BaCO₃ and CuO. A stoichiometric amount of the cationic ratio of Y : Ba : Cu = 1 : 2 : 3, respectively was stirred in distilled water and then well mixed for 12 hr by a high power sonifier. The solution was dried at 90 C until well-mixed powders were obtained. The powders were then ground for 2 hr and sintered at 900 C for 20 hr and then annealed at 550 C for 15 hr in an oxygen-enriched environment. The last process was repeated. A series of polycrystalline composite samples of (100-x) YBa₂Cu₃O_{7-δ} + x Ni (where x = 0, 2.5, 5, 10 and 15 wt.%) was grounded and then pressed into pellets. The composite pellets were sintered at 900 C for 20 hr and cooled to 550 C where they kept for 15 hr at an oxygen-enrichment environment condition.

2.2. Characterization process

The X-rays diffraction (XRD) patterns of the samples were made using X-ray Diffractometer (PANalytical, Netherlands) with Cu K α radiation ($\lambda=1.54 \text{ \AA}$). The diffraction data were collected over the diffraction angle range $2\theta = 10^\circ\text{--}80^\circ$ with settings of 40 mA current and 40 kV. Microstructure pictures were taken using a scanning electron microscope (SEM) Unit (Quanta 250 FEG, USA) with an Energy Dispersive X-ray spectroscopy (EDX) analyzer with accelerating voltage 30 kV.

2.3. Measurements of temperature-dependent-ultrasonic attenuation coefficient α

The attenuation coefficient α of the ultrasonic longitudinal wave was measured as a function of temperature by employing the ultrasonic pulse echo system. By measuring the maximum amplitude of the first and second pulse echoes (A_1, A_2) and by knowing the sample thickness K , α could be defined using the following equation,

$$\alpha = \frac{20}{2K} \ln \frac{A_1}{A_2} \left(\frac{\text{dB}}{\text{cm}} \right) \dots \dots \dots (1)$$

The components of the used ultrasonic pulse echo system are

- 1- Ultrasonic flaw detector (Karl Deutsch-ECHOGRAPH 1080, Germany): for driving piezoelectric transducers and measuring peaks of the attenuated echoes bouncing off the opposite faces of the sample.
- 2- Quartz transducers of frequencies 4, 10 and 20 MHz.
- 3- Low-temperature varnish (CRYO BITZ-ICEIES03, England): for coupling transducers with sample at low temperatures $\geq 40 \text{ K}$.

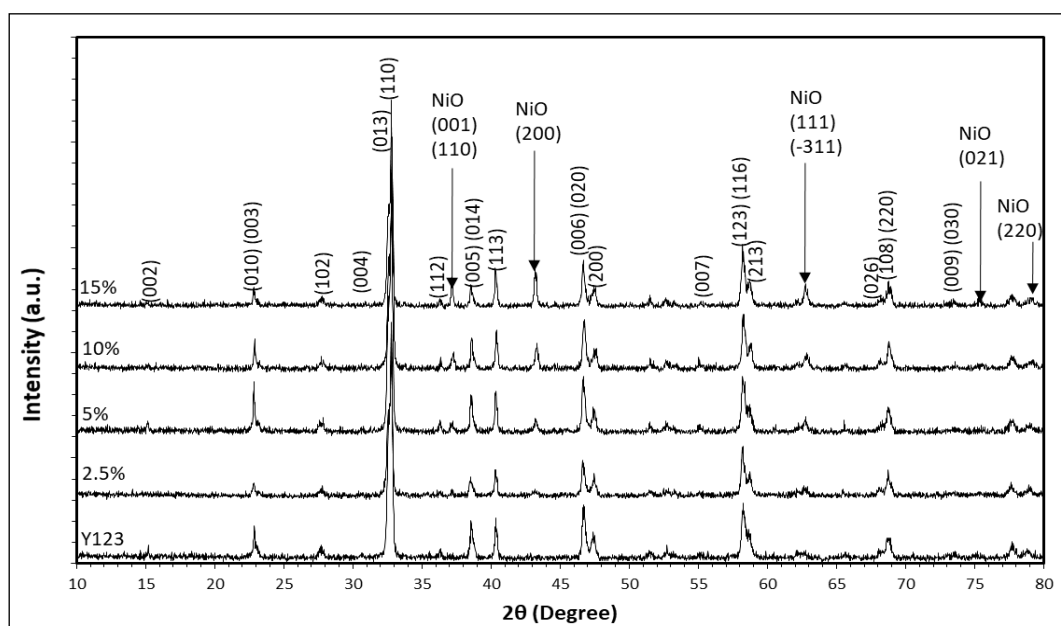
The temperature of the samples was varied by a cooling system that works from room temperature down to 40 K with a temperature resolution of $\pm 0.1 \text{ K}$. The system has the facility to fix the temperature of the sample at a certain degree. The components of the cooling system are:

- 1- Cryo- compressor (IBARA-531- 120, JAPAN) working with helium
- 2- Cooled head (JANIS-CCS- 100EB, USA) supplied with a suitable holder
- 3- Vacuum pump (EDWARDS-RVB, England)
- 4- Temperature controller (LAKESHORE-321- Autotuning, USA) supplied with silicon diode thermo-sensor and heating element to measure and control the temperature of the sample. Temperature accuracy with calibrated sensor is $\pm 0.3 \text{ K}$ at 77 K and $\pm 0.2 \text{ K}$ at 300 K.

III. RESULTS AND DISCUSSIONS

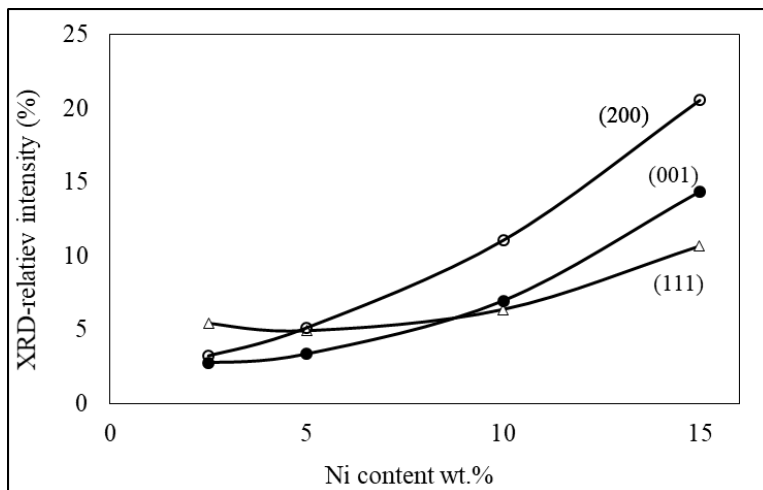
3.1. X-rays diffraction (XRD) analysis

Fig. 1 shows the XRD patterns of the samples Y123 + x Ni ($x = 0, 2.5, 5, 10$ and $15 \text{ wt.}\%$). The results show a predominant phase of Y123 with orthorhombic Pmmm symmetry. Monoclinic phase of NiO is clearly observed with growing peaks by increasing Ni metal content.



: XRD Patterns of (100-x) Y123 + x Ni samples ($x = 0, 2.5, 5, 10, 15 \text{ wt.}\%$)

Fig. 2 shows the relative intensity at (001), (200) and (111) planes of NiO monoclinic phase as a function of Ni wt.%. It is clearly shown that more number of diffraction is coming from these planes by increasing Ni metal content. This confirms the agglomerations or segregations of large quantities of Ni (in form of NiO) into patches or dots.



3.2. Microstructural and EDX analysis

Fig. 3 shows SEM graphs of the samples Y123 + x Ni (x = 0, 2.5, 5, 10 and 15 wt.%), in addition to EDX analysis for the positions marked in graphs. The insertions show more magnification at determined positions. From SEM images, two distinct features are observed; the first one is all samples exhibit randomly oriented grains (with varied sizes) in all directions with the presence of pores between them. Secondly is segregation of NiO in patches. EDX analysis for the positions X1 to X3 shows all the compositional elements. The EDX analysis of position X1 shown in fig. 3(a) proves the elemental composition of pure Y123. Whilst the EDX analyses of positions X2 and X3 shown in fig. 3(b) indicate the low and high concentration of Ni outside and inside the “blackish” patch, respectively. In other words, Ni is segregated into NiO blackish patches and its concentration decreases as moving away from those patches as indicated by the linear EDX analysis of the line shown in fig. 3(d). It can be extrapolated that Ni ions move away from NiO patches in three-dimensional percolation process through Y123 crystal lattice substituting for the Cu-sites [2-5].

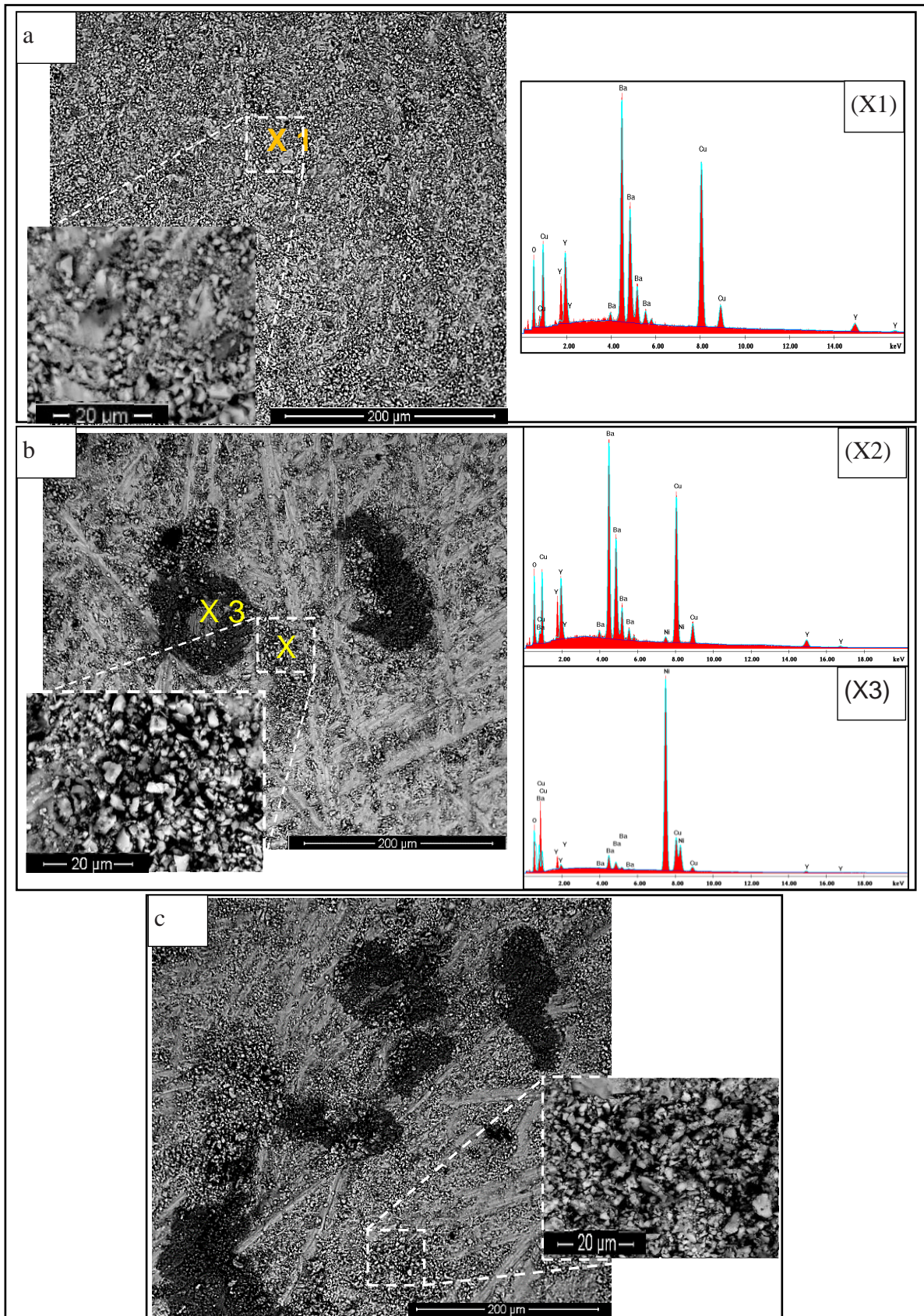


Fig. 3: see the next page.

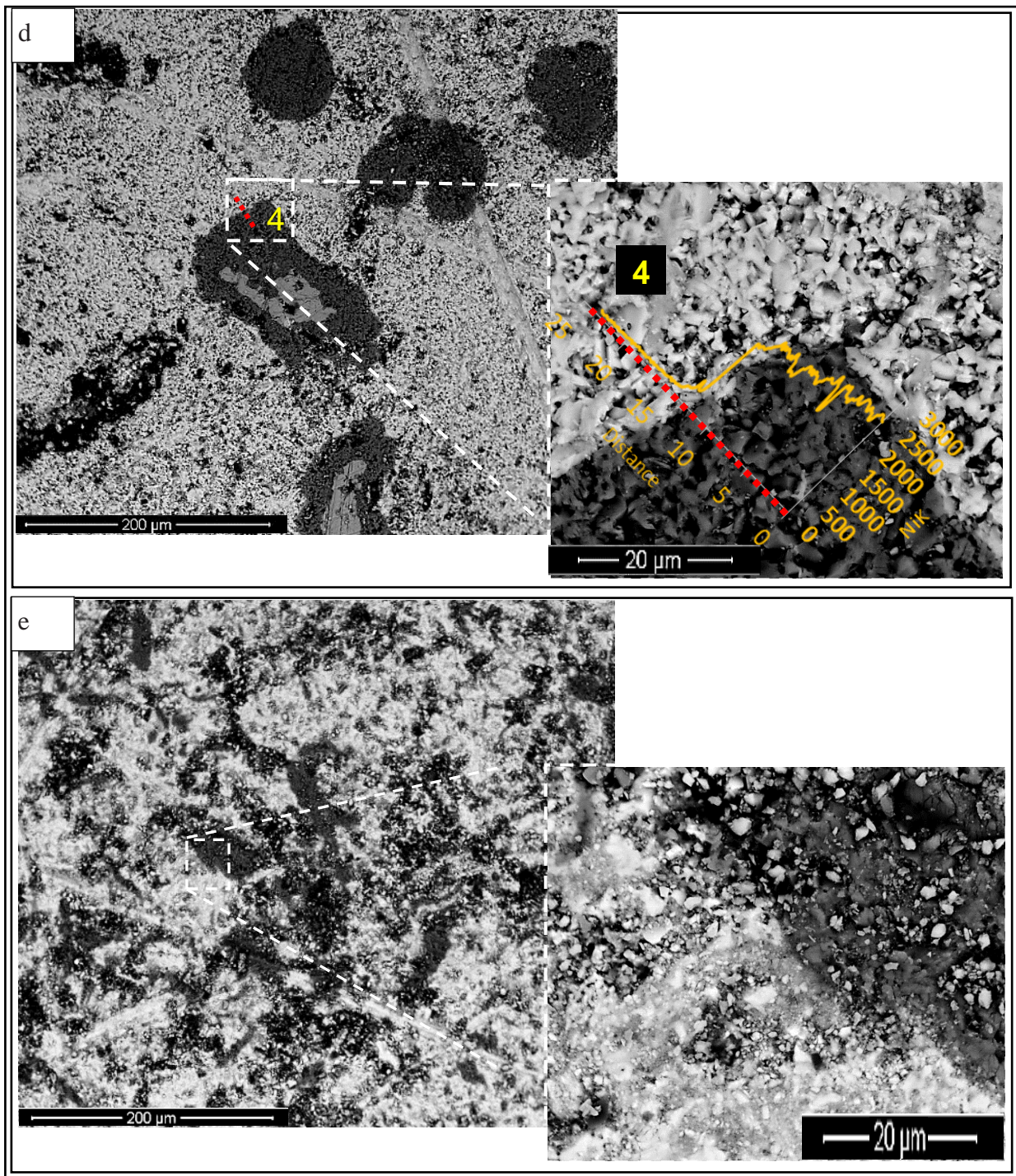
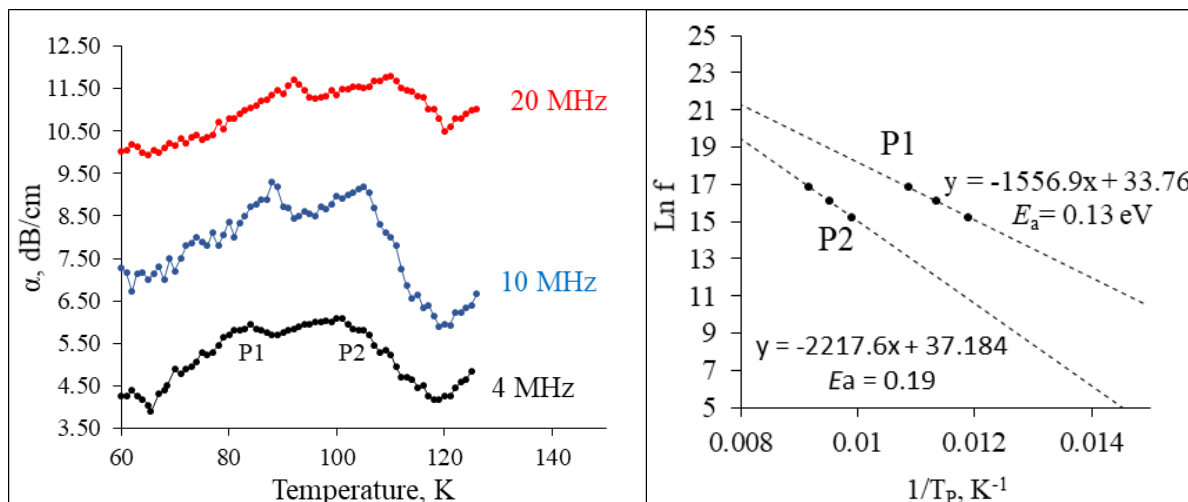


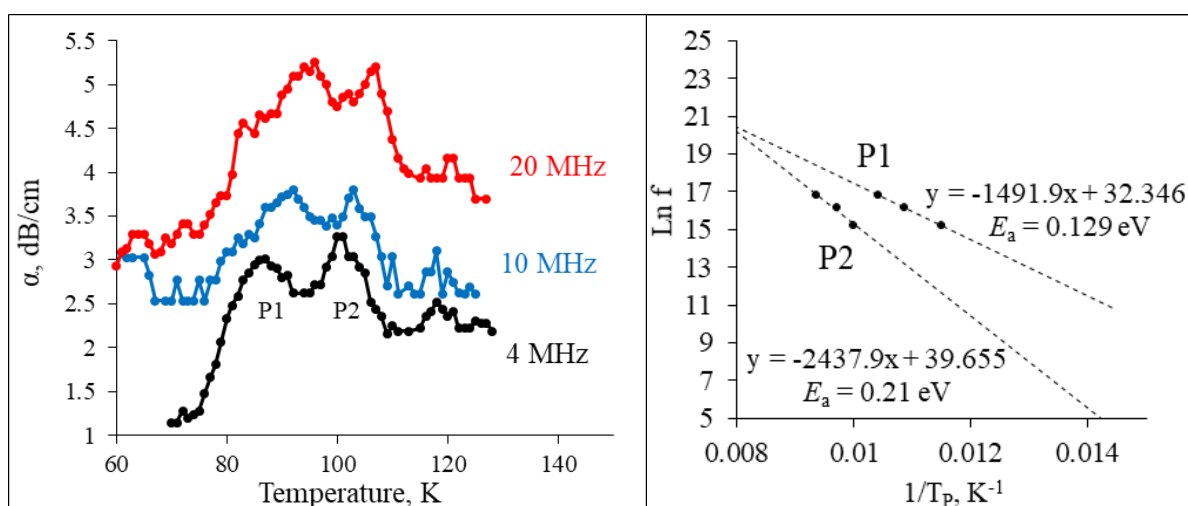
Fig. 3: SEM micrographs of the samples Y123 + x Ni composites (x = 0, 2.5, 5, 10 and 15 wt.%) marked as (a), (b), (c), (d) and (e) respectively and EDX analysis of Y123 and 2.5 wt.% Ni samples at positions marked as, X1, X2, X3 in addition to linear EDX analysis of 10 wt.% Ni sample at line marked as \4.

3.3. Measurements of temperature-dependent-ultrasonic attenuation

Fig. 4 shows the measurements of ultrasonic longitudinal attenuation α at frequencies 4 MHz, 10 MHz and 20 MHz in the temperature range 120-60 K for the samples (a) Y123 and (b) Y123+2.5 wt.% Ni. The remaining samples have the same characteristics.



(a)



(b)

Fig. 4: Temperature-dependent attenuation measurements at three different frequencies, 4 MHz, 10 MHz and 20 MHz in (a) Y123 and (b) Y123 + 2.5 wt.% Ni, adjacent to each graph the Arrhenius plots ($\ln(f)$ vs. $1/T_p$) of the relaxation rates obtained from attenuation peaks P1 and P2.

Increasing the frequency further caused the peak position to shift to a higher temperature. This behavior is a characteristic of a relaxation process for sound wave attenuation [19, 20]. Peaks (P1 & P2) are associated with the superconducting transition, though they have nothing to do with superconductivity. In other words, P1 & P2 are not due to electron-phonon interaction. They are due to a relaxation mechanism of a perturbed two-energy-level system that may be associated to magnetic excitations of spin fluctuations in CuO_2 planes and in Cu-O chains [21, 22]. The propagation of the sound wave through the sample introduces periodic deformations in the lattice that results in a periodic variation of the energy difference between energy levels of Cu^{+2} ions [20]. As a result, the electron populations of each energy level will change as well. The periodic perturbation of electron transitions will affect the net magnetic moments of the Cu^{+2} ions that affect the long-range AF correlations in the CuO_2 plane. The instantaneous return of overpopulated and underpopulated electron levels to their equilibrium states after disappearing the mechanical deformations is delayed. Therefore, the relaxation process of the electrons to their equilibrium states is out of phase with respect to the traveling wave. The energy of the sound wave is thus dissipated or attenuated.

The attenuation coefficient (α) can be described by the following expression [20],

$$\frac{\alpha}{\alpha_{max}} = 2 \frac{\omega\tau(T)}{1 + \omega^2\tau^2(T)} \dots \dots \dots (2)$$

Where α_{max} is the maximum attenuation at angular frequency ω , and τ (T) is the characteristic relaxation time, which is falling with temperature and behaves as Arrhenius relation as following [23],

$$\tau(T) = \tau_0 e^{(E_a/kT)} \dots \dots \dots (3)$$

where E_a is an activation energy of the relaxation process associated with the ultrasonic attenuation peak, τ_0 is the inverse of the attempt frequency f_0 , k is the Boltzmann constant, and T is absolute temperature. At α_{max} , i.e. at each peak, $\omega\tau_p = 2\pi f\tau_p = 1$

$$\left. \begin{aligned} \therefore \tau_p(T_p) &= \tau_0 e^{(E_a/kT_p)} \\ \therefore 2\pi f\tau_0 e^{(E_a/kT_p)} &= 1 \\ \therefore f &= \frac{e^{(-E_a/kT_p)}}{2\pi\tau_0} \end{aligned} \right\} \dots \dots \dots (4)$$

$$\therefore \ln f = \frac{-E_a}{kT_p} + \ln \frac{1}{2\pi\tau_0} \dots \dots \dots (5)$$

For different frequencies and by using equation (5), the activation energies can be determined as shown in fig. 4. The activation energies of the relaxation processes associated with the attenuation peaks P1 and P2 are about 0.13 eV and 0.2 eV, respectively. We note that the activation energy controlling process of peak P1 is about 0.13 eV which is very close to the AF exchange energy J [24]. This means the relaxation process that results in rising peak P1 is associated with magnetic excitations of spin magnetic moment fluctuations in CuO_2 planes, as discussed above. Measurements of Xu et al. [25] on sinter-forged-Y123 samples revealed the presence of a small peak close to T_C at 70 K, where the used 12 MHz longitudinal waves propagating parallel to a , b plane induced stresses or excitations within CuO_2 planes. This means there is a coupling mechanism between sound wave and magnetic spin moments in the CuO_2 planes. The present results have satisfied these points. The effect of Ni^{2+} -presence in CuO_2 plane on AF correlations is very clear on suppressing the peak P1, as shown in fig. 5. Ni^{2+} has the electron configuration $4s^0 3d^8$, so its magnetic moment is supposed to be of $S=1$ (1.73 μB), but the effective moment is less than that value [2, 26]. The magnetic moment has two components; $3d_{x^2-y^2}^1$ and $3d_{z^2-r^2}^1$ [26]. Ni^{2+} substituting Cu plane sites retains the magnetic moment component of Ni $3d_{z^2-r^2}^1$ that will be almost isolated because the magnetic channels between the Ni $3d_{z^2-r^2}^1$ spin and neighboring host Cu $3d_{x^2-y^2}^1$ spins are very weak. The isolated spin magnetic moment Ni $3d_{z^2-r^2}^1$ may weakly disturb the AF exchange correlations due to that of Ni $3d_{x^2-y^2}^1$ [27-31]. Ni^{2+} at CuO_2 plane is therefore a magnetic scatterer, to be precise Ni^{2+} barely perturbs AF correlations in the low-Ni-concentration-Y123. Rising number of Ni^{2+} ions in Cu-plane sites has a dominant impact on suppressing AF correlations in CuO_2 plane. Fig. 5(f) shows the decrements in height of P1 with Ni content. At low Ni ≤ 2.5 wt.%, P1 is nearly unchanged, but a further increase of Ni, starting from 2.5 wt.%, results in a clear reduction in its height. From the measurements of the superconducting transition temperature T_C , shown in fig. 5(f), we found T_C decreases as Ni content is increased. This tendency coincides with that of P1 and such similarity suggests there might be some correlation between superconductivity and the relaxation species of P1.

Almond et al. [22] discussed in detail the possibility of magneto-acoustic coupling of the elastic wave with spin moments in the Cu-O chains. They concluded that the proposed magnetic excitations could have energy separations close to activation energy of process associated with P2. As most of Ni ions stays preferentially at CuO_2 planes, therefore the height of P2 doesn't change much till 10 wt.% Ni. However, abrupt decrease occurs in height of P2 at 15 wt.% Ni, fig. 5(g). This may be due to the increasing perturbation on magnetic excitations in the Cu-O chains as a result of probable existence of Ni ions in these chains at high Ni doping of 15 wt.%.

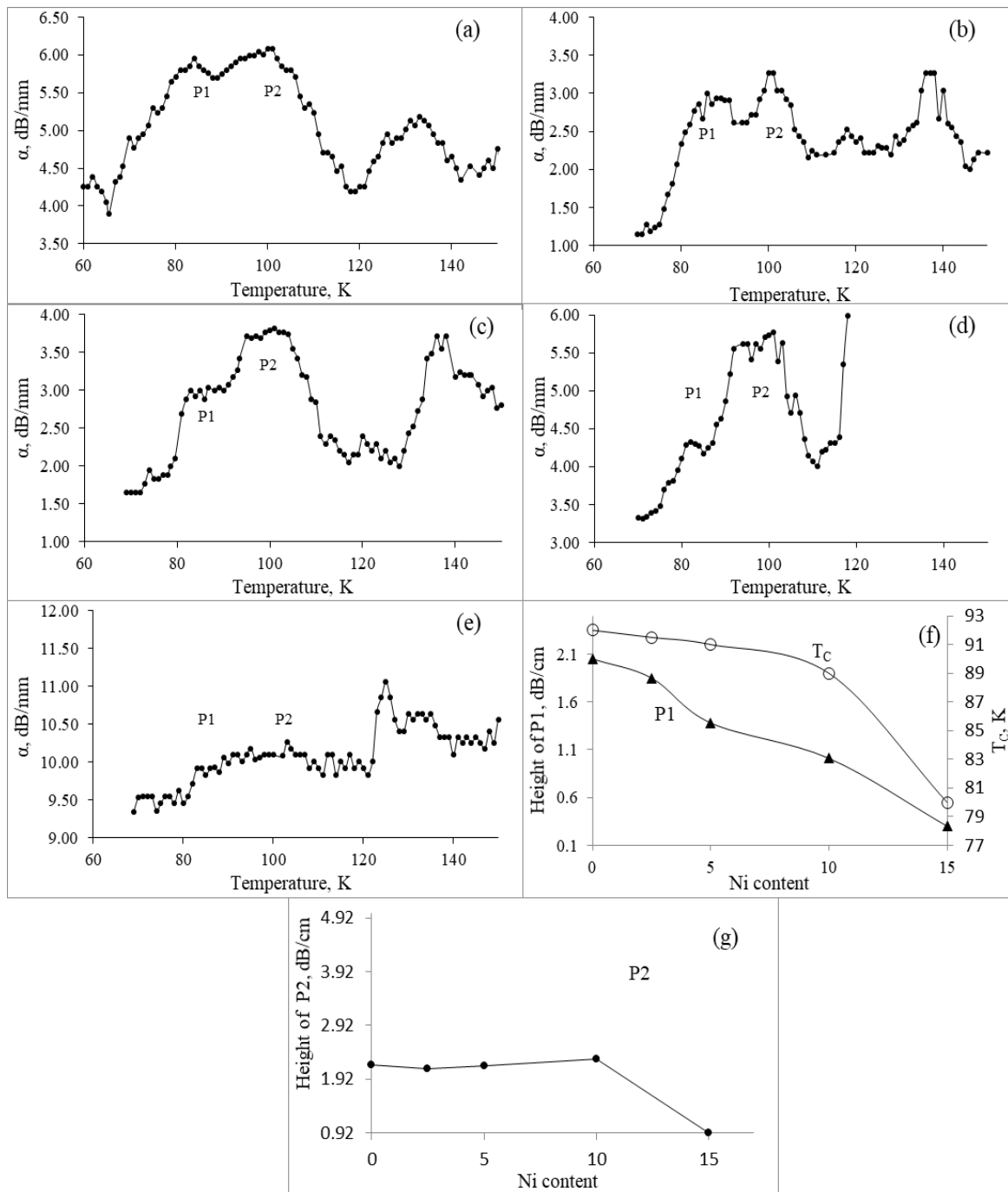


Fig. 5: The attenuation measurements of the ultrasonic longitudinal waves at frequency 4MHz for samples (a) Y123, (b) 2.5, (c) 5, (d) 10, (e) 15 wt.% Ni, (f) height of peak P1 & T_C vs. Ni content and (g) height of peak P2 vs. Ni content.

IV. CONCLUSION

The ultrasonic attenuation coefficient of superconductor Y123 exhibited two close peaks (P1, P2) in the vicinity of superconducting transition temperature. The activation energies of the relaxation processes associated with the attenuation peaks P1 and P2 are found very close to the AF exchange energy J . P1 and P2 are associated with magnetic excitations of spin magnetic moment fluctuations in Cu-O planes and chains, respectively. Ni^{2+} -doping in CuO_2 planes was found to affect the height of P1. The weak perturbation of AF correlations due to low-Ni-concentration-Y123 had small effect on P1 height. However, further increase of Ni^{2+} resulted in a clear reduction in its height. Further substitution of Ni^{2+} in Cu sites are thought to have increasing

effect on AF superexchange correlations that are playing very effective role of forming Zhang-Rice (ZR) singlets and their pairing mechanisms. Increase of Ni²⁺ ions in CuO₂ planes and their resulted dynamic processes affect clearly the superconducting properties including T_C. Decrease of T_C as Ni content is of tendency coinciding with that of P1 and such similarity confirms the presence of the correlation between superconductivity and the relaxation species of P1. The height of P2 did not change much up to high Ni doping (about 10 wt.% Ni). This may be due to the existence of Ni ions preferentially at CuO₂ planes. However, abrupt decrease occurred in height of P2 at 15 wt.% Ni. This may be due to the increasing perturbation on magnetic excitations in the Cu-O chains as a result of probable existence of Ni ions in these chains at high Ni doping of 15 wt.%.

References

- [1] G. Xiao, M.Z. Cieplak, D. Musser, A. Garvin, F.H. Stretz, C.L. Cien, J.J. Rhyne and J.A. Gotaas, Significance of plane versus chain sites in high-temperature oxide superconductors, *Nature*, **332**, 1988, 238-240.
- [2] W. Kang, H.J. Schulz, D. Jerome, S.S.P. Parkin, J.M. Bassat and Ph. Odier, Effects of Ni-to-Cu substitution on the properties of the high-T_C superconductor La_{1.85}Sr_{0.15}CuO_{4-y}, *Physical Review B*, **37**, 1988, 5132-5135.
- [3] R.S. Howland, T.H. Geballe, S.S. Laderman, A.F. Colbrie, M. Scott, J.M. Tarascon and P. Barboux, Determination of dopant site occupancies in Cu-substituted YBa₂Cu₃O_{7-δ} by differential anomalous x-ray scattering, *Physical Review B*, **39**, 1989, 9017-9027.
- [4] C.Y. Yang, A.R. Moodenbaugh, Y.L. Wang, Y. Xu, S.M. Heald, D.O. Welch, M. Suenaga, D.A. Fischer and J.E.P. Hahn, X-ray absorption near-edge studies of substitution for Cu in YBa₂(Cu_{1-x}M_x)₃O_{7-δ} (M=Fe, Co, Ni, and Zn), *Physical Review B*, **42**, 1990, 2231-2241.
- [5] F. Bridges, J.B. Boyce, T. Claeson, T.H. Geballe and J.M. Tarascon, Local structure about Ni atoms in Ni-substituted YBa₂Cu₃O_{7-δ}, *Physical Review B*, **42**, 1990, 2137-2142.
- [6] E.W. Hudson, K.M. Lang, V. Madhavan, S.H. Pan, H. Eisaki, S. Uchida and J.C. Davis, Interplay of magnetism and high-T_C superconductivity at individual Ni impurity atoms in Bi₂Sr₂CaCu₂O_{8+δ}, *Nature*, **411**, 2001, 920-924.
- [7] D. Haskel, E.A. Stern, V. Polinger and F. Dogan, Ni-induced local distortions in La_{1.85}Sr_{0.15}Cu_{1-y}Ni_yO₄ and their relevance to T_C suppression: An angular-resolved XAFS study, *Physical Review B*, **64**, 2001, 104510.
- [8] Y. Itoh, S. Adachi, T. Machi, Y. Ohashi, and N. Koshizuka, Ni-substituted sites and the effect on Cu electron spin dynamics of YBa₂Cu_{3-x}Ni_xO_{7-δ}, *Physical Review B*, **66**, 2002, 134511.
- [9] X. Gaojie, M. Zhiqiang, W. Yu and Z. Yuheng, Two-dimensional hole localization induced by Zn, Ni, and Mg dopings in Cu sites in La_{1.85}Sr_{0.15}Cu_{1-x}M_xO_y, *Journal of Superconductivity* **10**, 1997, 13-18.
- [10] K.B. Lyons, P.A. Fleury, J.P. Remeika, A.S. Cooper and T.J. Negran, Dynamics of spin fluctuations in lanthanum cuprate, *Physical Review B*, **37**, 1988, 2353-2356.
- [11] G. Blumberg, P. Abbamonte, M.V. Klein, W.C. Lee, D.M. Ginsberg, L.L. Miller and Z. Zibold, Resonant two-magnon Raman scattering in cuprate antiferromagnetic insulators, *Physical Review B*, **53**, 1996, R11930-R11933.
- [12] G. Blumberg, M. Kang, M.V. Klein, K. Kadowaki and C. Kendziora, Evolution of Magnetic and Superconducting Fluctuations with Doping of High-T_C Superconductors, *Science*, **278**, 1997, 1427-1432.
- [13] F.C. Zhang and T.M. Rice, Effective Hamiltonian for the superconducting Cu oxides, *Physical Review B*, **37**, 1988, 3759-3761.
- [14] K.J. Sun, W.P. Winfree, M.F. Xu, B.K. Sarma and M. Levy, Frequency-dependent ultrasonic attenuation of YBa₂Cu₃O₇, *Physical Review B*, **38**, 1988, 11988-11991.
- [15] K.J. Sun, M. Levy, B.K. Sarma, P.H. Hor, R.L. Meng, Y.Q. Wang and C.W. Chu, Ultrasonic measurements on polycrystalline YBa₂Cu₃O₇, *Physics Letters A*, **131**, 1988, 541-544.
- [16] T. Takanohashi, Ultrasonic study of lattice instability in high-T_C superconductors, *Physica B*, **219-220**, 1996, 182-185.
- [17] T. Deng, L. Zhang, H. Gu, Z. Xiao and L. Chen, Ultrasonic studies on high T_C superconductor YBa₂Cu₃O_{7-x}, *Chinese Physics Letters*, **5**, 1988, 461-464.
- [18] W. Yening, S. Huimin, Z. Jinsong, X. Ziran, G. Min, N. Zhongmin and Z. Zhifang, Study on the anomalies of YBa₂Cu₃O_{9-x} between 90-260 K by elasticity measurements and x-ray diffraction, *Journal of Physics C: Solid State Physics*, **20**, 1987, L665-L668.
- [19] R.B. Lindsay, *Mechanical Radiation* (New York: McGraw-Hill, 1960).
- [20] M. Levy, M.F. Xu, B.K. Sarma and K.J. Sun, Ultrasonic Propagation in Sintered High-T_C Superconductors, in M. Levy (Ed.), *Ultrasonics of High-T_C and Other Unconventional Superconductors*, Physical Acoustics Volume XX, (Academic Press, Inc., 1992) 247-248.
- [21] Q.M. Zhang, X.N. Ying, A. Li, W.M. Chen, X.S. Xu, B.Q. Li and Y.N. Wang, Investigation on three internal friction peaks at low temperature in Ni doped YBa₂Cu₃O_{7-δ}, *Physica C: Superconductivity*, **341-348**, 2000, 601-602.
- [22] D.P. Almond, M.W. Long and G.A. Saunders, Anelastic relaxation evidence of very low activation energy processes in superconducting YBa₂Cu₃O_{7-x}: magnetic chain excitations?, *Journal of Physics: Condensed Matter*, **2**, 1990, 4667-4674.
- [23] D.P. Almond, A Rationalisation of the Diversity in the Elastic Response of Polycrystalline Superconducting Oxides, in M. Levy (Ed.), *Ultrasonics of High-T_C and Other Unconventional Superconductors*, Physical Acoustics Volume XX, (Academic Press, Inc., 1992) 420-421.
- [24] P. Bourges, H. Casalta, A.S. Ivanov and D. Petitgrand, Superexchange Coupling and Spin Susceptibility Spectral Weight in Undoped Monolayer Cuprates, *Physical Review Letters*, **79**, 1997, 4906-4909.
- [25] M.-F. Xu, D. Bein, R.F. Wiegert, B.K. Sarma, M. Levy, Z. Zhao, S. Adenwalla, A. Moreau, Q. Robinson, D.L. Johnson, S.-J. Hwu, K.R. Poeppelmeier and J.B. Ketterson, Ultrasonic attenuation measurements in sinter-forged YBa₂Cu₃O_{7-δ}, *Physical Review B*, **39**, 1989, 843-846.
- [26] P. Mendels, H. Alloul, G. Collin, N. Blanchard, J.F. Marucco, J. Bobroff, Macroscopic magnetic properties of Ni and Zn substituted YBa₂Cu₃O_y, *Physica C: Superconductivity*, **235-240**, 1994, 1595-1596.

- [27] K. Ishida, Y. Kitaoka, N. Ogata, T. Kamino, K. Asayama, J.R. Cooper, and N. Athanassopoulou, Cu NMR and NQR Studies of Impurities-Doped $\text{YBa}_2(\text{Cu}_{1-x}\text{M}_x)_3\text{O}_7$ (M=Zn and Ni), *Journal of the Physical Society of Japan*, 62, 1993, 2803-2818.
- [28] G.V.M. Williams, J.L. Tallon and R. Dupree, NMR study of magnetic and nonmagnetic impurities in $\text{YBa}_2\text{Cu}_4\text{O}_8$, *Physical Review B*, 61, 2000, 4319-4325.
- [29] Y. Sidis, P. Bourges, H.F. Fong, B. Keimer, L.P. Regnault, J. Bossy, A. Ivanov, B. Hennion, P.G. Picard, G. Collin, D.L. Millius and I.A. Aksay, Quantum Impurities and the Neutron Resonance Peak in $\text{YBa}_2\text{Cu}_3\text{O}_7:\text{Ni}$ versus Zn, *Physical Review Letters*, 84, 2000, 5900-5903.
- [30] Y. Tokunaga, K. Ishida, Y. Kitaoka and K. Asayama, Novel relation between spin-fluctuation and superconductivity in Ni substituted high- T_C cuprate $\text{YBa}_2\text{Cu}_3\text{O}_7:\text{Cu}$ NQR study, *Solid State Communications*, 103, 1997, 43-47.
- [31] M.Z. Cieplak, S. Guha, H. Kojima, P. Lindenfelf, G. Xiao, J.Q. Xiao and C.L. Chien, Metal-insulator transition in $\text{La}_{1.85}\text{Sr}_{0.15}\text{CuO}_4$ with various substitutions for Cu, *Physical Review B*, 46, 1992, 5536-5547.

Hesham A. Afifi "Temperature-dependent ultrasonic attenuation of superconducting composite Y123+Ni at low temperature." IOSR Journal of Applied Physics (IOSR-JAP) , vol. 10, no. 4, 2018, pp. 60-69.